

Tropospheric temperature gradient and its relation to the South and East Asian precipitation variability

B. H. Vaid¹ · X. San Liang¹

Received: 15 January 2015 / Accepted: 26 May 2015 / Published online: 31 May 2015
© Springer-Verlag Wien 2015

Abstract Using the NCEP–DOE AMIP-2 daily re-analysis data sets, the tropospheric temperature (TT) changes over East Asia for the period 1988–2010 are analyzed. It is found that on the layer-averaged TT between 1000 and 400 mb, there exist two centers, one sitting over Mongolia, another over Tibet. An index, called TT index, is defined as the difference between the TT over these centers. The TT index is observed to reflect the circulation anomaly through thermal wind relation. A significant increase in magnitude is identified after 1999; the trend, however, reveals a much milder slope in comparison to that prior to 1999. It is found that the TT index is highly correlated to the South and East Asian precipitation variability. It is related to other monsoon indices in that it takes a lead of approximately 15 days; computation with a newly developed rigorous causality analysis reveals unambiguously a one-way causality from the TT index to the latter. That is to say, we could have identified something that may help better predict the precipitation variability.

1 Introduction

The tropospheric temperature (hereafter TT) is very important in climate research in that it may form one of the most dramatic climate change signals in the recent climate

record (Randel et al. 2009; Emanuel et al. 2013; Vecchi et al. 2013). It significantly influences the climate variability over East Asia and other parts of the globe (Yu et al. 2004; Wu 2005; Yu and Zhou 2007; Emanuel 2010; Vecchi et al. 2013; Zhang and Zhou 2013). For example, the upper (around 300 hPa) TT cooling during 1958–2001, a result of the interaction between the troposphere and stratosphere, has been shown to weaken the East Asian summer monsoon (Yu et al. 2004); the upper tropospheric variations are observed to weaken the northward progression of the southerly monsoon winds, resulting in a mid–lower Yellow River valley (34°N–40°N) drought and excessive rain in the Yangtze River valley (Yu and Zhou 2007); Wu (2005) showed that the TT decreases over East Asia and the African monsoon region weaken the Indian summer monsoon circulation during the mid-1960s, whereas the tropospheric warming over the tropical area from the Indian Ocean and western Pacific are observed to cause the weakening of the Indian summer monsoon circulation appeared in the late 1970s. Also, the TT seems to have crucial impacts on the tropical storm activities through changing its potential intensity (Emanuel 2010; Vecchi et al. 2013). Besides, its anomalous behavior has been associated with exceptional summer rainfalls, resulting in floods or droughts (Parthasarathy et al. 1990; Yu et al. 2004; Zhang and Zhou 2012), and exerting large influence on the populous Asian region.

Whereas the role that the TT plays on our earth system has been recognized, the details of the TT variability over the East Asia were not fully explored yet, and the associated possible mechanism remains elusive. This is particularly the case for the monsoon system which we will be studying henceforth. For instance, on interannual time-scales, it has been found that the south Asian monsoon rainfall has a strong and positive correlation with the pre-

Responsible Editor: L. Gimeno.

✉ B. H. Vaid
bakshi32@gmail.com

¹ School of Marine Sciences, Nanjing University of Information Science and Technology, Nanjing, China

monsoon spring tropospheric temperature anomaly (Verma 1980; Parthasarathy et al. 1990; Singh and Chattopadhyay 1998). Obviously, the TT contains much information on climate variability in general, and the East Asia climate variability in particular. However, in comparison to the related research over other regions, the study of the TT variation over East Asia is far from enough.

Moreover, the present study intends to bring out the association of the meridional gradient of the TT and precipitation over the South and East Asia. It is observed that the deep tropospheric heating cannot be elucidated by the classical land–ocean contrast model involving surface temperature gradient forces (Schneider and Lindzen 1977), as it can only explain shallow circulation. Webster et al. (1998) observed that the deep Asian monsoon circulation is a manifestation of the meridional gradient of the deep tropospheric heat and may be efficaciously represented by the meridional gradient of the TT. In response to such a heat source (Gill 1980; Rodwell and Hoskins 1996), a large scale cyclonic circulation is generated above the planetary boundary layer (PBL). Sensible heating over the Tibetan Plateau during the pre-monsoon period plays not only a crucial role in setting up the deep heating in the northern location (Yanai et al. 1992; Li and Yanai 1996), but also an instrumental role in the meridional gradient of the TT. In addition, heat advection associated with quasi-stationary planetary waves can also influence the temperature of the northern part and hence the meridional gradient of the TT. The new findings here indicate that these TT gradients are observed to affect the precipitation variability of both the South and East Asia monsoon. So, therefore, it is very essential to study the meridional gradient of the TT and its variations. In all due fairness, perhaps, we can say that meridional gradient TT over the East Asia contains much information on climate variability, and its evaluation should be useful for climate detection and ascription. In short, the present study is intended to unveiling of the tropospheric temperature gradient over East Asia and its association with South and East Asia precipitation variability. Besides, the TT variation during different climate phase is delineated. In the following, we first list the data source, and then give a brief presentation of the results. This study is summarized in Sect. 4.

2 Data used

We use for our purpose the National Center for Environmental Prediction (NCEP)–DOE AMIP 2 reanalysis daily data sets for air temperature, sea surface level pressure, geopotential height, horizontal and meridional wind fields, and relative humidity (Kanamitsu et al. 2002), which are provided by the NOAA/OAR/ESRL PSD, Boulder,

Colorado, USA, and are available from their website at <http://www.esrl.noaa.gov/psd/>. The precipitation data are from Asian Precipitation-Highly-Resolved Observational Data Integration Towards Evaluation (APHRODITE's) of Water Resources; the APHRODITE project produces for the Asian region highly resolved (0.25° by 0.25°), state-of-the-art daily precipitation data, primarily with measurements from a rain-gauge-observation network (Yatagai et al. 2012).

3 Results

With the daily NCEP–DOE AMIP-2 data, we average the air temperature between 400 and 1000 mb, and call the resulting field tropospheric temperature (hereafter TT). Besides, we distinguish two periods for our analysis: the period 1988–1998 (PRE99) and the period 1999–2010 (POST99). The periods PRE99 and POST99 are chosen, as the first leading empirical orthogonal function (EOF) mode of the POST99 tropical Pacific SSTA has shown maximum warming is the central Pacific (around 150°W), whereas the PRE99 EOF1 mode shows a warming in the eastern Pacific. In other words, from PRE99 to POST99, the EOF mode of the tropical Pacific SSTA has shifted its maximum warm center of the eastern Pacific to the central Pacific (Xiang et al. 2013; Chung and Li 2013). This study provides the consistent picture of the role of the TT variation over the East Asia and its association with South and East Asian monsoon. The dynamical regime of the monsoon variability perhaps seems to be dominated by the TT variation over the East Asia. Figure 1 shows (a) the JJAS-averaged TT for the period PRE99, (b) same TT but for the period POST99, and (c) the difference between the above two (POST99 minus PRE99). The TT over regions Long. = 89°E – 128°E , Lat. = 42°N – 55°N (hereafter region I) and Long. = 79°E – 100°E , Lat. = 30°N – 39°N (hereafter region II), respectively, marked in Fig. 1 are analyzed. As can be seen, substantial difference is observed in the period PRE99 and POST99, particularly over regions I and II. In other words, it is found that on the layer-averaged TT between 1000 and 400 mb, there exist two centers, one sitting over Mongolia, another over Tibet. Since horizontal temperature gradients induce thermal winds, we subtract the TT over region I from that over region II, and refer to it as TT gradient. This gradient, as implied by the thermal wind relation, plays an important role in driving the circulation; we henceforth make it an index, called the “TT index”. The TT gradient or index is plotted in Fig. 2, respectively, for PRE99 and POST99.

A careful comparison of Fig. 2a, b shows that the index has experienced a change in pattern since PRE99. This distinguishes the role of the TT during the two different

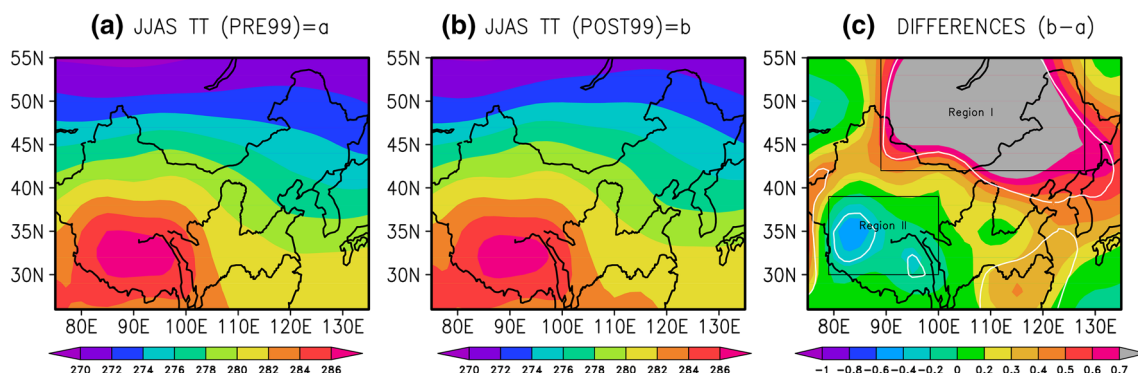
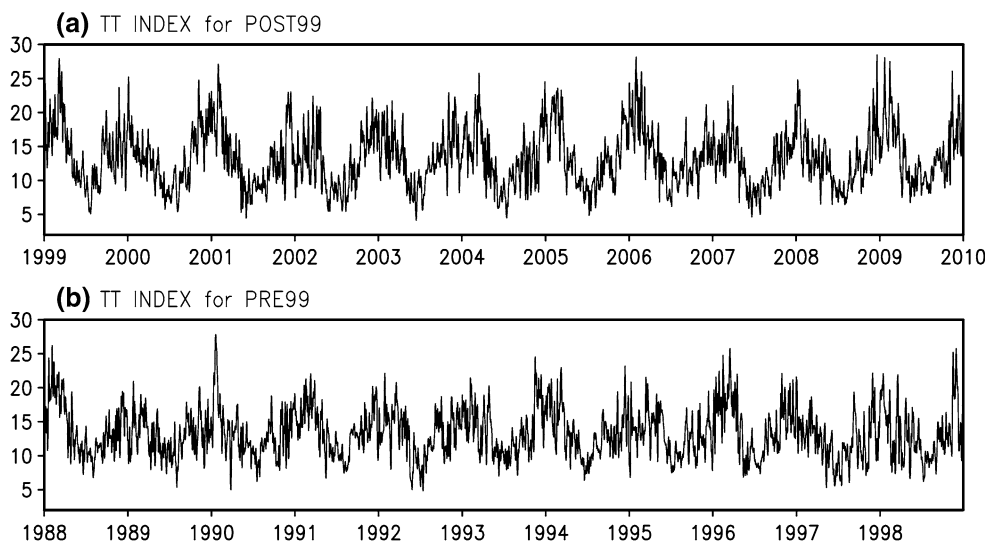


Fig. 1 a JJAS TT (in k) for PRE99, b JJAS TT for POST99 and c JJAS differences, POST99 minus PRE99. The regions enclosed in white contours are significantly different from zero at a 99 % level

Fig. 2 a TT index for the period POST 99 (daily data from 1999–2010). b TT index for the period PRE99 (daily data from 1988–1998)



climate phases PRE99 and POST99. First, it is observed that the variance has significantly increased; the amplitude in Fig. 2a is clearly larger than that in Fig. 2b. Second, the TT is observed to be decreasing during the periods in question, but the decreasing rates are very different. Figure 3 shows, respectively, the linear trends of the TT for periods PRE99 and POST99 (Fig. 3a, b). Clearly the trends are quite different: in comparison to the latter, the former has a much steeper slope. To see whether the slope difference is significant, we find that, at a 85 % confidence level, the two slopes are -2.09 ± 0.74 and -0.50 ± 0.86 , respectively. In other words, they lie within $[-2.83, -1.35]$ and $[-1.36, 0.36]$. As these ranges do not overlap, the two indeed significantly differ at a 85 % confidence level. Also shown are the equivalent potential temperature (θ_e) (region II minus region I) over 1000 mb minus that over 700 mb for the two periods (Fig. 3c, d). In this case, the two slopes have opposite signs, echoing the above slope difference in an enhanced way. Obviously, the TT is decreasing, but the decreasing trend has slowed down after 1999. However, the

amplitude of the variability (hence the variance) has been increased ever since.

It is of interest to see what a circulation pattern the TT change may result in. For this purpose, we construct the JJAS horizontal wind shear (200–850 mb) averaged for the PRE99 and POST99 periods, and then subtract the former from the latter. The resulting difference field is drawn in Fig. 4. We identified that TT variation during the POST99 seems to be associated with the distinctive circulation feature. The closed loop circulation structures are clearly seen over the regions I and II. A conspicuous feature is the anticyclonic circulation over region I. Geopotential height analysis for the two periods also results in similar structures (not shown).

The TT variability is observed to bear a high correlation with the precipitation variability over East and South Asia (Fig. 5). This actually is implied from the distinct loop structures in Fig. 1c. To illustrate, let T be the temperature between two pressure levels P_0 and P_1 (here 1000 and 400 mb), R the universal gas constant, f the Coriolis parameter, then

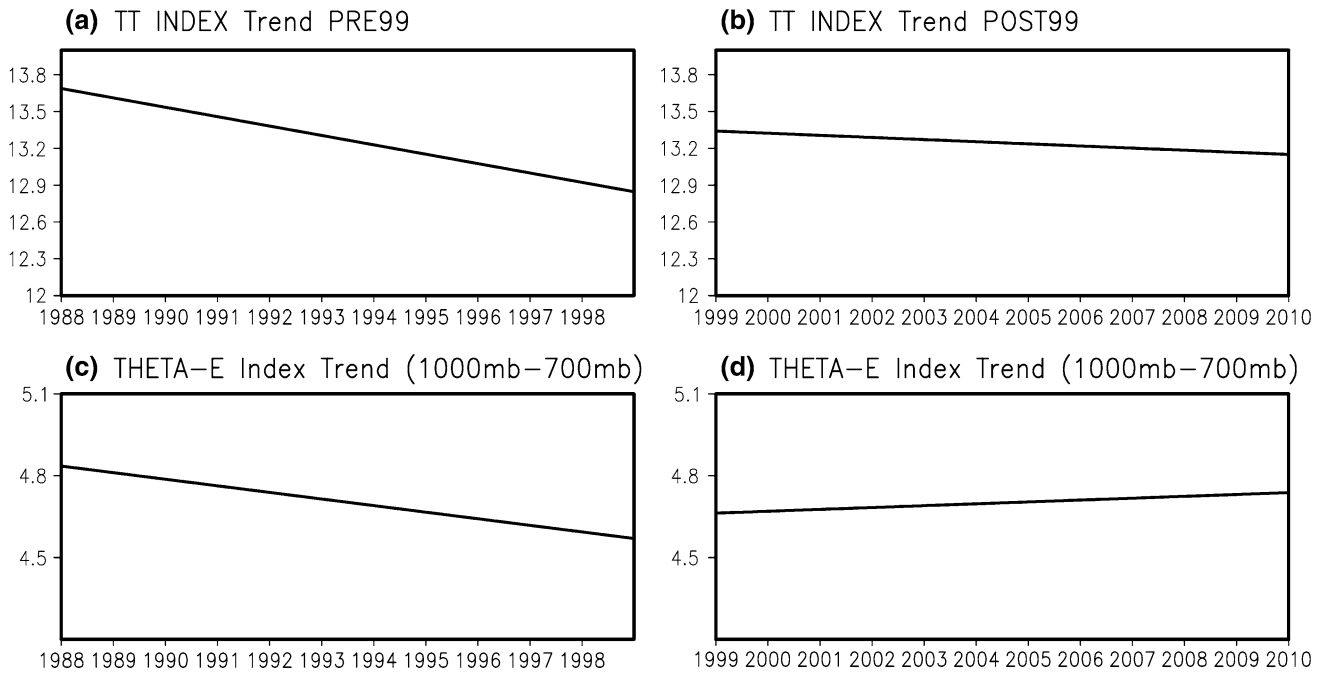


Fig. 3 **a** TT index trend for PRE99. **b** TT index trend for POST99. **c** Equivalent potential temperature (region II minus region I) over 1000 mb minus that over 700 mb for the period PRE99. **d** Same as

(c), but for POST99. The trend computation is with the data through the whole year (not just for JJAS)

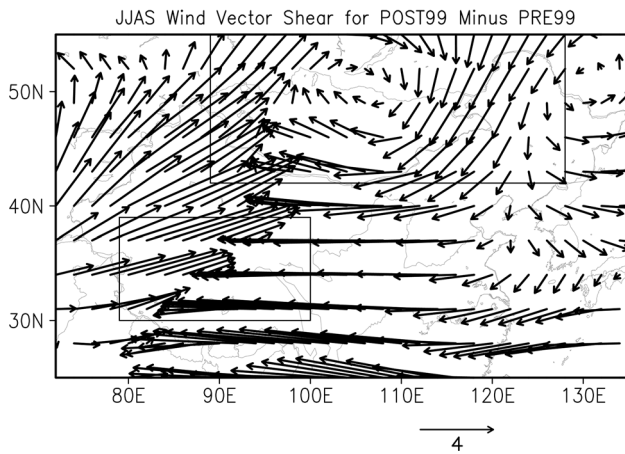


Fig. 4 The JJAS wind vector shear difference (period POST99 minus PRE99)

$$\frac{\partial V_g}{\partial \ln P} = \frac{-R}{f} \hat{k} \times \nabla_p T,$$

and hence the thermal wind shear between P_0 and P_1 is, by integration,

$$\begin{aligned} V_T &= V_g(P_1) - V_g(P_0) = -\frac{R}{f} \int_{P_0}^{P_1} (\hat{k} \times \nabla_p T) d \ln P \\ &= -\frac{R}{f} \nabla_p \langle T \rangle \ln \left(\frac{P_0}{P_1} \right), \end{aligned}$$

where ∇_p signifies the gradient operator on the pressure surface. This formula says that, in the Northern Hemisphere, if we face downstream, the warm air is on our right-hand side. The structure in Fig. 1c, therefore, implies a southeasterly wind anomaly in POST99. As the southeasterly brings humidity from the ocean, China should have experienced a wetter POST99 period, which is indeed true as an observed precipitation trend over China (area averaged over 73°E:136°E, 20°N:50°N) ranges from 1.62 to 1.74 and 1.45 to 2.1 during PRE99 and POST99, respectively.

To see more about the precipitation–TT index relation, we plot in Fig. 5a, b, the standard deviations of precipitation variability for the periods PRE99 and POST99; also plotted is their difference (Fig. 5c). Generally speaking, the deviation is large over the South while it is small over the Northwest. This general pattern remains the same before and after 1999, but the change over the transition period differs from region to region. As shown in Fig. 5c, the variabilities over Southern China, Tibet, and Indo-China Peninsula have been enhanced, while those over Indian, Northeastern China, and the Yangtze Valley have been reduced ever since. For the sake of comparison, we regress these variabilities onto the TT index (the regression coefficients are significant at a 99 % confidence level), and draw the resulting structures in Fig. 5d, e, respectively. Obviously, except for those over Southeast China, Japan, and Korea, the precipitation variability over the vast region can

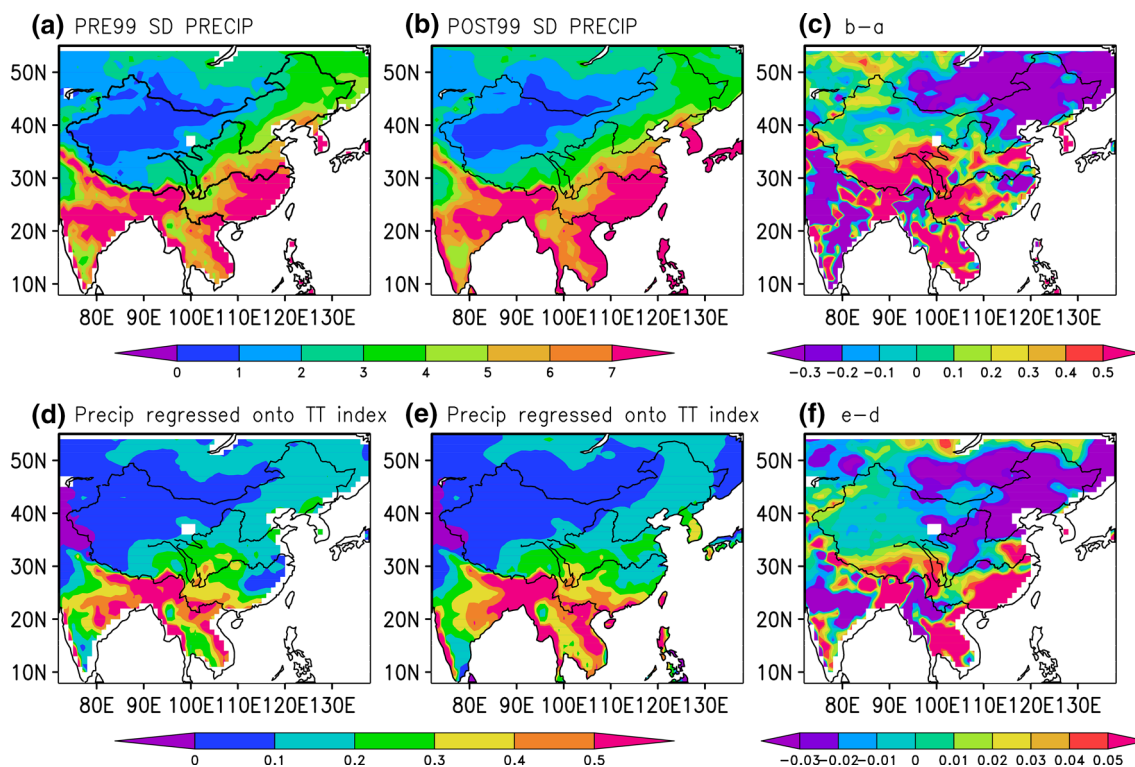


Fig. 5 Upper panel standard deviation of the precipitation variability: **a** PRE99, **b** POST99, **c** difference $b - a$. Lower panel precipitation variability regressed (statistically significant at a 99 % confidence level) onto the TT index: **d** PRE99, **e** POST99, **f** difference $e - d$

be well explained by the TT index. If we compare Fig. 5c, f (difference between Fig. 5e, d), the similarity is even better. We are therefore confident that the TT gradient or TT index is directly related to the precipitation over Asia.

Considering the role that monsoon plays in the precipitation over Asia, the above TT–precipitation relation suggests some association of the TT gradient with the summer monsoon system. The Asian monsoon system includes the South Asian monsoon and the East Asian monsoon which begins over South China Sea. Previously, to characterize the broad-scale feature of the former, Webster and Yang (1992) introduced a circulation index which is defined as a time-mean zonal wind (U) shear between 850 and 200 mb, written U200–U850, averaged over South Asia from the equator to 20°N and from 40°E to 110°E (hereafter WYI region). For the latter, similarly the same U shear over 105°E–120°E, 5°N–20°N (hereafter region III) has been proposed (Liang and Shang-sen 2002). Now let us see how our TT index is related to these traditional U shear indices. Figure 6a shows the TT index climatology, and Fig. 6b shows, respectively, the area-averaged U shear climatologies (U200–U850) over region III (marked by open circle) and over region WYI (by plus sign). Apparently, the

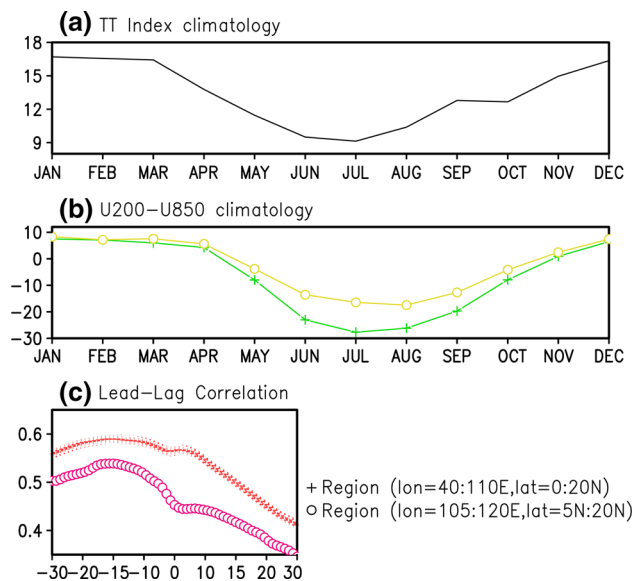


Fig. 6 **a** The TT index climatology for the period 1988–2010. **b** Area-averaged U shear (m/sec) climatology (U200–U850) over region III (open circle) and region WYI (plus sign). **c** Lead-lag correlation between the TT index and the U shear index over region III (open circle) and that over WYI (plus sign); a negative number means that the TT index takes lead

TT index in Fig. 6a looks similar in structure to those in Fig. 6b, and indeed, they are correlated to a significant extent. A lead-lag correlation analysis, however, shows that there is actually an advance in phase in the TT index variability (Fig. 6c). Here the lead-lag correlation analysis is conducted between the TT index series (for period 1988–2010) and the area-averaged time series of the velocity shear U200–U850 (zonal velocity at 200 and 850 hPa, respectively). We have tried both the U shear over region III (105°E–120°E, 5°N–20°N) and region WYI (90°E–110°E, 0°N–20°N), and the results are similar. That is to say, the TT gradient takes lead of about 15 days, with respect to both the WYI and the South China Sea monsoon index.

The lead seems that the TT index may embed some ingredients that cause the monsoon. But, of course, (time-delayed) correlation does not necessarily imply causation, which has long been debated in statistics, physics, and even philosophy. But here dynamically it is understandable that the TT gradient may cause the U shear process—the thermal relation reads that a temperature gradient drives a circulation. To see whether this is indeed true, we further apply a recently rigorously developed causality analysis (Liang 2014; Liang 2013) to this problem, and examine the causation in a quantitative way. This analysis uses information flow to quantify the causality between time series. Suppose we have two series X_1 and X_2 , then, as proved in Liang (2014), the rate of information flowing from the latter to the former, $T_{2 \rightarrow 1}$, can be very easily estimated with the following formula (units: nats per unit time):

$$T_{2 \rightarrow 1} = \frac{C_{11}C_{12}C_{2,d1} - C_{12}^2C_{1,d1}}{C_{11}^2C_{22} - C_{11}C_{12}^2},$$

where C_{ij} is the sample covariance between X_i and X_j , and $C_{i,dj}$ the sample covariance between X_i and $\dot{X}_j = \frac{X_{j,t+1} - X_j}{\Delta t}$ (Δt is the time stepsize). If $|T_{2 \rightarrow 1}|$ is nonzero, X_2 is causal to X_1 ; if not, it is noncausal. This remarkably concise formula, which is derived from first principles after some simplification, has been validated with touchstone examples, and has been applied with success to many realistic problems in different disciplines.

We compute the information flow rates and list the results in the following table. Take for an

	Causality in terms of information flow rate (nats/day)
TT → WYI U shear	0.241
WYI U shear → TT	0.0591
TT → III U shear	0.272
III U shear → TT	0.0335

example the information flow from between the TT index and the U shear over the WYI region. The forward flow rate is 0.241 nats/day, while the reverse flow rate is 0.0591 nats/day, almost negligible in comparison to the forward one. We have performed a 90 % significant test, which shows that the former is significant, while the latter is not. Same is true with those between the TT index and the U shear over region III. The causation between the TT index and the U shear is therefore essentially one way, i.e., the former causes the latter. An unambiguous one-way causality has been quantitatively revealed, substantiating what we observed in the above.

4 Concluding remarks

Our analysis with the daily mean NCEP reanalysis data and the APHRODITE precipitation data has shown the 1000–400 mb layer-averaged tropospheric temperature (TT) has distinctly different evolutionary patterns before and after 1999, which we refer to as PRE99 and POST99, respectively. The POST99–PRE99 TT difference reveals two closed centers, one over Mongolia and another over Tibet. We have averaged the TT over these centers and taken difference to make an index, called TT gradient or TT index. This TT index is important in that it reflects the circulation anomaly through thermal wind relation. It has also shown to be highly correlated to the precipitation variability over most part of China, Indian, and the Indo-China Peninsula; the implied southeasterly wind anomaly agrees with the observed wetter climate since 1999. Compared to the traditional indices of the South Asia and South China Sea summer monsoon, the TT index is found to be 15 days ahead. The high 15 day-lead correlation between the TT index and the traditional indices indicates that the former may be the cause while the latter the effect, and this is indeed the case when tested with a newly rigorously developed quantitative causality analysis. That is to say, we could have identified something that may help better predict the precipitation variability. In a sense, we can say that the TT index is a precursor of the summer monsoon; it may help us issue in advance hazard warning correspondingly.

Acknowledgments The comment from an anonymous referee is appreciated. This research was partially supported by the National Science Foundation of China (NSFC) under Grant No. 41276032, and by Jiangsu Government through the “Specially-Appointed Professor Program” (Jiangsu Chair Professorship) to XSL. Thanks are due to the NCEP–DOE AMIP 2 reanalysis group and the APHRODITE’s team for providing the data.

References

- Chung PH, Li T (2013) Interdecadal relationship between the mean state and El Niño types. *J Clim* 26(2):361–379
- Emanuel K (2010) Tropical cyclone activity downscaled from NOAA-CIRES reanalysis, 1908–1958. *J Adv Model Earth Syst*. doi:[10.3894/JAMES.2010.2.1](https://doi.org/10.3894/JAMES.2010.2.1)
- Emanuel K, Solomon S, Folini D, Davis S, Cagnazzo C (2013) Influence of the tropical tropopause layer cooling on Atlantic hurricane activity. *J Clim* 26:2288–2301
- Gill AE (1980) Some simple solutions for heat-induced tropical circulation. *Q J R Meteorol Soc* 106:447–462
- Kanamitsu M, Ebisuzaki W, Woollen J, Yang SK, Hnilo JJ, Fiorino M, Potter GL (2002) NCEP–DOE AMIP-II reanalysis (R-2). *Bull Am Meteorol Soc* 83:1631–1643
- Li C, Yanai M (1996) The onset and interannual variability of the Asian summer monsoon in relation to land–sea thermal contrast. *J Clim* 9:358–375
- Liang XS (2013) The Liang–Kleeman information flow: theory and applications. *Entropy* 15:327–360
- Liang XS (2014) Unraveling the cause–effect relation between time series. *Phys Rev E* 90:052150
- Liang J, Shang-sen WU (2002) A study of southwest monsoon onset date over the South China Sea and its impact factors. *Chin J Atmos Sci* 26(6):829–844
- Parthasarathy B, Rupa Kumar K, Sontakke NA (1990) Surface and upper air temperatures over India in relation to monsoon rainfall. *Theor Appl Climatol* 42:93–110
- Randel WJ et al (2009) An update of observed stratospheric temperature trends. *J Geophys Res* 114:D02107. doi:[10.1029/2008JD010421](https://doi.org/10.1029/2008JD010421)
- Rodwell MJ, Hoskins BJ (1996) Monsoons and dynamics of deserts. *Q J R Meteorol Soc* 122:1385–1405
- Schneider E, Lindzen R (1977) Axially symmetric steady state models of the basic state of instability and climate studies. Part I: linearized calculations. *J Atmos Sci* 34:23–279
- Singh GP, Chattopadhyay J (1998) Relationship of tropospheric temperature anomaly with Indian southwest monsoon rainfall. *Int J Climatol* 18:759–763
- Vecchi GA, Fueglistaler S, Held IM, Knutson TR, Zhao M (2013) Impacts of atmospheric temperature trends on tropical cyclone activity. *J Clim* 26:3877–3891
- Verma RK (1980) Importance of upper tropospheric thermal anomalies for long-range forecasting of Indian summer monsoon activity. *Mon Weather Rev* 108:1072–1075
- Webster PJ, Yang S (1992) Monsoon and ENSO: selectively interactive systems. *Q J R Meteor Soc* 118:877–926
- Webster PJ, Magana VO, Palmer PN, Shukla J, Tomas RT, Yanai M, Yasunari T (1998) Monsoons: processes, predictability and the prospects of prediction. *J Geophys Res* 103:14451–14510
- Wu BY (2005) Weakening of Indian summer monsoon in recent decades. *Adv Atmos Sci* 22(1):21–29
- Xiang B, Wang B, Li T (2013) A new paradigm for the predominance of standing Central Pacific Warming after the late 1990s. *Clim Dyn* 41(2):327–340
- Yanai M, Li CF, Song ZS (1992) Seasonal heating of the Tibetan Plateau and its effects on the evolution of the Asian Summer Monsoon. *J Meteorol Soc Jpn* 70:319–351
- Yatagai AK, Kamiguchi K, Arakawa O, Hamada A, Yasutomi N, Kitoh A (2012) APHRODITE: constructing a long-term daily gridded precipitation dataset for Asia based on a dense network of rain gauges. *Bull Am Meteorol Soc*. doi:[10.1175/BAMS-D-11-00122.1](https://doi.org/10.1175/BAMS-D-11-00122.1)
- Yu R, Zhou T (2007) Seasonality and three-dimensional structure of the interdecadal change in East Asian monsoon. *J Clim* 20:5344–5355
- Yu R, Wang B, Zhou T (2004) Tropospheric cooling and summer monsoon weakening trend over East Asia. *Geophys Res Lett* 31:L22212. doi:[10.1029/2004GL021270](https://doi.org/10.1029/2004GL021270)
- Zhang L, Zhou T (2012) The interannual variability of summer upper-tropospheric temperature over East Asia. *J Clim* 25:6539–6553
- Zhang L, Zhou T (2013) A comparison of tropospheric temperature changes over China revealed by multiple datasets. *J Geophys Res Atmos* 118:4217–4230